AD-A277 329

(2)

OFFICE OF NAVAL RESEARCH

GRANT: N00014-89-J-1178

TECHNICAL REPORT NO. 64

R&T CODE: 413Q001-05

POST-CALIBRATION CORRECTION FOR ROTATING-ANALYZER ELLIPSOMETER WITH OPTICAL FIBER BUNDLE DETECTION SYSTEM

BY

S.Y. KIM, L. SPANOS, E.A. IRENE

DEPARTMENT OF CHEMISTRY
CB#3290 VENABLE
UNIVERISTY OF NORTH CAROLINA
CHAPEL HILL, NC 27599-3290

DTIC
ELECTE
MAR 24 1994
S E D

SUBMITTED TO:

JOURNAL OF APPLIED OPTICS

REPRODUCTION IN WHOLE OR IN PART IS PERMITTED FOR ANY PURPOSE OF THE UNITED STATES GOVERNMENT.

THIS DOCUMENT HAS BEEN APPROVED FOR PUBLIC RELEASE AND SALE; ITS DISTRIBUTION IS UNLIMITED.

Accesion For	
NTIS CRA&I	☒
DTIC TAB	☐
Unannounced	☐
Justification	
By	
Distribution /	
Availability Codes	
Dist	Avail and / or Special
A-1	

94-09186

94 3 23 039

REPORT DOCUMENTATION PAGE

Form Approved
OMB No 0704-0188

Public reporting burden for this collection of information is estimated to average 1 hour per response, including the time for reviewing instructions, searching existing data sources, gathering and maintaining the data needed, and completing and reviewing the collection of information. Send comments regarding this burden estimate or any other aspect of this collection of information, including suggestions for reducing this burden to Washington Headquarters Services, Directorate for information Operations and Reports, 1215 Jefferson Davis Highway, Suite 1204, Arlington, VA 22202-4302, and to the Office of Management and Budget, Paperwork Reduction Project (0704-0188), Washington, DC 20503

1. AGENCY USE ONLY (Leave blank)	2. REPORT DATE	3. REPORT TYPE AND DATES COVERED
	March 15, 1994	Technical Report #64

4. TITLE AND SUBTITLE
Post-calibration Correction for Rotating-Analyzer Ellipsometer with Optical Fiber Bundle Detection System

5. FUNDING NUMBERS
N00014-89-J-1178

6. AUTHOR(S)
S.Y. Kim, L. Spanos, E.A. Irene

7. PERFORMING ORGANIZATION NAME(S) AND ADDRESS(ES)
Department of Chemistry
University of North Carolina
CB #3290 Venable & Kenan Labs
Chapel Hill, NC 27599-3290

8. PERFORMING ORGANIZATION REPORT NUMBER
N00014-89-J-1178
Technical Report #64

9. SPONSORING/MONITORING AGENCY NAME(S) AND ADDRESS(ES)
Department of Navy
Office of Naval Research
800 North Quincy Street
Arlington, VA 22217-5000

10. SPONSORING/MONITORING AGENCY REPORT NUMBER

11. SUPPLEMENTARY NOTES
Submitted to Journal of Applied Optics

12a. DISTRIBUTION/AVAILABILITY STATEMENT
Reproduction in whole or in part is permitted for any purpose of the United States Government. This document has been approved for public release and sale; its distribution is unlimited.

12b. DISTRIBUTION CODE

13. ABSTRACT *(Maximum 200 words)*

Spectroscopic ellipsometry with a rotating-analyzer operated without a dark room is examined. The effect of the residual linear polarization at the output of an optical fiber bundle upon the ellipsometric constants is critically analyzed. The fraction of the linear polarization and the rotation angle of the polarization axis inside the optical fiber are the two key elements of the post-calibration correction. The spectral dependence of the calibration constants is corrected.

DTIC QUALITY INSPECTED 1

14. SUBJECT TERMS	15. NUMBER OF PAGES
Spectroscopic, ellipsometry, optical fiber bundle	16. PRICE CODE

17. SECURITY CLASSIFICATION OF REPORT	18. SECURITY CLASSIFICATION OF THIS PAGE	19. SECURITY CLASSIFICATION OF ABSTRACT	20. LIMITATION OF ABSTRACT
Unclassified	Unclassified	Unclassified	

Post-calibration correction for rotating-analyzer ellipsometer with optical fiber bundle detection system

Sang Youl Kim, Lycourgos Spanos, and Eugene A. Irene
Department of Chemistry, The University of North Carolina
Chapel Hill, North Carolina 27599-3290

Spectroscopic ellipsometry with a rotating-analyzer operated without a dark room is examined. The effect of the residual linear polarization at the output of an optical fiber bundle upon the ellipsometric constants is critically analyzed. The fraction of the linear polarization and the rotation angle of the polarization axis inside the optical fiber are the two key elements of the post-calibration correction. The spectral dependence of the calibration constants is corrected.

Introduction

Spectroscopic ellipsometry (SE) has been widely used for surface and thin film analyses.[1-3] A rotating-analyzer (RA) type SE system is popular because of its simplicity in design.[4,5] Many RA type SE systems have the same basic configuration: a white light source - monochromator - fixed polarizer - sample - rotating analyzer - light detection system. Some SE systems have slightly modified configuration such as, white light source - rotating polarizer (RP) - sample - fixed analyzer - monochromator - and

photo-detection system[6] and is called an RP type SE system. The compensator is not always used because of calibration difficulties over a spectral range. No commercial achromatic compensator is presently available. RP and RA type SE systems are in principle identical in operation, wavelength scan range, accuracy in data, data collection speed, and in many other aspects. But in practice, these SE systems have both strong and weak points. Both are photometric, and as such have inherent weaknesses in measuring the linearly polarized light. The RA type SE system is ideally operated in a dark room or at least special precautions need to be taken to block the collection of stray light. Also for the RA type SE system, the background noise treatment is one of the most important considerations in the calibration procedure. The RP type SE, on the other hand, can be operated without special precautions in room light, but the inherent partial polarization of the light source needs to be optically removed or corrected for (possibly in software) before the rotating polarizer. One way to accomplish this is to use a fixed polarizer in between the light source and the rotating polarizer.[7] This solution has the disadvantage of adding one more optical element into the system and thus increasing the inherent complexity of an otherwise simple SE system. The procedures associated with optical alignment, calibration, sample alignment, and the data collection are all affected. Another possible configration is to use the RA system but with an optical fiber bundle in the photo-detection system placed between the rotating analyzer and the monochromator, yielding the

configuration: white light source - fixed polarizer - sample - rotating analyzer - optical fiber - monochromator - photo-detection system. The multimode optical fiber will depolarize linear polarized incident light. This configuration can be used in room light, and the inherent polarization of the light source is not important. The negligibly small contribution from the room light can be measured and substracted from the signal level. The present work deals with characterizing the depolarizing action of the fiber bundle. If the depolarization is incomplete, there will be a leakage of the linearly polarized light and the effect on the ellipsometric constants has been analyzed. The detection of this leaky linear polarization and the procedure to make corrections to the measured ellipsometric constants is presented.

RA Type SE System With An Optical Fiber Bundle

The RA SE system considered is shown schematically in Figure (1). As mentioned above, the optical fiber bundle is located between the rotating analyzer and the monochromator. Assuming that the depolarizing action of the optical fiber is complete, that is, that the light emerging from the optical fiber is randomly polarized, the electric field, E, impinging upon the photomultiplier tube in terms of Jones vectors is given as:

$$E = E_o \begin{bmatrix} 1 & 0 \\ 0 & 0 \end{bmatrix} \begin{bmatrix} cosA & sinA \\ -sinA & cosA \end{bmatrix} \begin{bmatrix} r_p & 0 \\ 0 & r_s \end{bmatrix} \begin{bmatrix} cosP & -sinP \\ sinP & cosP \end{bmatrix} \begin{bmatrix} 1 \\ 0 \end{bmatrix}$$
$$= E_o \begin{bmatrix} cosA \\ sinA \end{bmatrix} [r_p cosA cosP + r_s sinA sinP] \qquad (1)$$

where A and P are the analyzer and the polarizer angles, r_p and r_s are the Fresnel reflection coefficients of the p and s waves, respectively. Since the intensity of light is given by $E_xE_x^*+E_yE_y^*$, the intensity of the light can be written as follows:

$$I = I_o \left[1 + \frac{\tan^2\psi - \tan^2 P}{\tan^2\psi + \tan^2 P} \cos 2A + \frac{2 \tan P \cos\Delta \tan\psi}{\tan^2\psi + \tan^2 P} \sin 2A\right] \qquad (2)$$

where it is accepted that $r_p = r_s \tan\psi \exp(i\Delta)$. An RA type SE system measures the modulated intensity of light. The measured intensity variation can be written similar to Eqn. (2):

$$I = I_o [1 + \alpha \cos 2A + \beta \sin 2A] \qquad (3)$$

The coefficients α and β of the above trigonometric functions are obtained from Fourier analysis and the ellipsometric constants Δ and Ψ can be expressed in terms of the Fourier coefficients as:

$$\tan\psi = \tan P \sqrt{\frac{1 + \alpha}{1 - \alpha}} \qquad (4)$$

$$\cos\Delta = \frac{\beta}{\sqrt{1 - \alpha^2}} \qquad (5)$$

An optical fiber might be leaky in its depolarizing action, that is, a small fraction of the linearly polarized light might exist at the fiber bundle exit. Furthermore the polarization axis might experience some amount of rotation while propagating through the optical fiber. The electric field of this part of the linearly polarized light, after making several reflections from the mirrors and the grating inside the monochromator, can be found from the following relationship:

$$E_f = E_{fo}\begin{bmatrix} M_x & 0 \\ 0 & M_y \end{bmatrix}\begin{bmatrix} \cos(F-A) & \sin(F-A) \\ -\sin(F-A) & \cos(F-A) \end{bmatrix}\begin{bmatrix} 1 & 0 \\ 0 & 0 \end{bmatrix}\begin{bmatrix} cosA & sinA \\ -sinA & cosA \end{bmatrix} \times \begin{bmatrix} r_p & 0 \\ 0 & r_s \end{bmatrix}\begin{bmatrix} cosP & -sinP \\ sinP & cosP \end{bmatrix}\begin{bmatrix} 1 \\ 0 \end{bmatrix} \quad (6)$$

Where M_x and M_y are the reflection coefficients of the x and y components of the electric field after the reflections from the mirrors and the grating inside the monochromator. F is the rotation angle of the linearly polarized light inside the optical fiber. The coordinate system is chosen such that the electric field of the p-wave vibrates along the x-axis, and that of the s-wave along the y-axis. Eqn. (6) can then be written compactly as:

$$E_f = E_{fo}\begin{bmatrix} M_x\cos(F-A) \\ -M_y\sin(F-A) \end{bmatrix}[r_p cosA cosP + r_s sinA sinP] \quad (7)$$

Now, most of the linearly polarized light becomes unpolarized at the output of the optical fiber, hence only a relatively small

fraction of the linearly polarized light is assumed to propagate through the optical fiber with a possible rotation of the polarization axis. The total electric field at the photomultiplier can be written as follows:

$$E_t = E_{ot} \begin{bmatrix} cosA + \varsigma M_x cos(F-A) \\ sinA - \varsigma M_y sin(F-A) \end{bmatrix} [r_p cosA cosP + r_s sinA sinP] \qquad (8)$$

where ς is the fraction of the electric field of the linearly polarized light exiting the optical fiber. With this expression for the electric field, the light intensity at the photomultiplier is obtained from:

$$I_t = I_{ot} [1 + \alpha\, cos2A + \beta\, sin2A] [1 - \xi cos2(F-A) + 2\varsigma Re(M_y)\{ cos(F-A) tan\psi_M cos\Delta_M - sin(F-A) \}] \qquad (9)$$

where

$$\xi = - \frac{\varsigma^2 (tan^2\psi_M - 1)}{2 + \varsigma^2 (tan^2\psi_M + 1)} \qquad (10)$$

and $Re(M_y)$ is the real part of M_y and $M_x = M_y\, tan\psi_M\, exp(i\Delta_M)$. A closer look at the Eqn. (9) reveals that the effects of the leaky linear polarized light on the signal are twofold: i) the first order harmonic of A, which has no direct effect on α, β but possibly has some effect via optical alignment, ii) the second harmonic of A, which has a direct effect on the measured α, β. The latter term is linear in ξ. ξ is a positive quantity ($|M_y| \geq |M_x|$). If $|M_y| = |M_x|$ then ξ is zero, meaning that the combined effect of the

optical fiber and the monochromator is zero on α, β. Now since our primary concern is with α and β, only the second order harmonic term of A inside the second bracket of the right hand side of the Eqn. (9) is considered which yields for the intensity:

$$I_t = I_{ot} [1 + \alpha_{2m} cos2A + \beta_{2m} sin2A + \alpha_{4m} cos4A + \beta_{4m} sin4A] \qquad (11)$$

where α_{2m}, β_{2m}, α_{4m} and β_{4m} in Eqn. (11) represents the measured Fourier coefficients. The errors of the electronics which converts the photo-current into the analog signal and those of the A/D converter are not explicitly taken into account. A detailed discussion about this latter issue can be found elsewhere.[4,5] Comparing Eqn. (9) to Eqn. (11), the following relations between $(\alpha_{2m}, \beta_{2m})$ and (α, β) are obtained:

$$\alpha = \frac{\alpha_{2m} + \xi cos2F + \frac{1}{2}\xi^2 sin2F\,(\beta_{2m} cos2F - \alpha_{2m} sin2F)}{1 + \frac{1}{2}\xi\,(\alpha_{2m} cos2F + \beta_{2m} sin2F)} \qquad (12)$$

$$\beta = \frac{\beta_{2m} + \xi sin2F + \frac{1}{2}\xi^2 cos2F\,(\alpha_{2m} sin2F - \beta_{2m} cos2F)}{1 + \frac{1}{2}\xi\,(\alpha_{2m} cos2F + \beta_{2m} sin2F)} \qquad (13)$$

Correction Terms

Two correction elements can be found in Eqns.(12) and (13): ξ and F. Although ξ and F are the correction elements, ξcos2F and

ξsin2F are measured and used as the correction terms. ξcos2F and ξsin2F can be measured at straight through operation (STO). If one measures the ellipsometric constants at glancing incidence (the angle of incidence = 90°) without a sample, then both tanψ and cosΔ should be 1.0 (r_p=r_s) for an ideal system. Hence one can set α=cos2P and β=sin2P (Eqns. (4) and (5)) for an ideal system at STO. Implementing these conditions into Eqns. (12) and (13) and solving for ξcos2F and ξsin2F yields the following expressions:

$$\xi cos2F = \frac{-\alpha_{sto} + cos2P + \frac{1}{2} sin2P\,(\alpha_{sto} sin2P - \beta_{sto} cos2P)}{1 - \frac{1}{2}\,(\alpha_{sto} cos2P + \beta_{sto} sin2P)} \qquad (14)$$

$$\xi sin2F = \frac{-\beta_{sto} + sin2P - \frac{1}{2} cos2P\,(\alpha_{sto} sin2P - \beta_{sto} cos2P)}{1 - \frac{1}{2}\,(\alpha_{sto} cos2P + \beta_{sto} sin2P)} \qquad (15)$$

Here P is the polarizer angle and α_{sto} and β_{sto} are the STO-measured Fourier coefficients of cos2A and sin2A, respectively.

Experimental Procedures

The RA type SE system shown in Figure 1 has two arms that can be rotated such that the angle of incidence can be changed from ~45° to 90°. The angle of incidence can be read to the accuracy of 0.01°. On one arm is a 75W high pressure Xe-arc lamp, a set of low pass filters, an iris diaphram with an electrical shutter, a focusing lens made of vitreous silica, and a calcite Glan-Taylor

polarizer mounted on a manual rotator. The sample stage is at the center of the main body and the rotation axis of the two arms. On the other arm, another Glan-Taylor polarizer is mounted on the hollow axis of a rotating cylinder with an optical encoder (360 encodings/turn with TZ signal), an auto-collimating telescope, and an optical fiber bundle. At the other end of the optical fiber is attached a vitreous silica lens which collimates the output light from the optical fiber onto the entrance slit of the monochromator (0.25m) which has a triple grating turret. An end-on photomultiplier tube is mounted at the exit slit of the monochromator. The photocurrent from the photomultiplier tube is fed into a current-to-voltage converter, an amplifier and a voltage follower. Output from the voltage follower is directed to the analog-digital converter and to the host computer. Most operations of the SE system are carried out under computer control, such as engaging the shutter on and off for the measurement of background, which is substracted from the measured signal intensity at each measurement, wavelenth scanning according to initial settings, and adjusting the photomultiplier high voltage to keep the signal at a constant level. Placing low-pass filters at lower photon energies and changing polarizer angle when necessary are done manually. The host computer is an IBM-PC compatable and the programs for data collection are done with ASYST 4.0.

For conventional SE operation, calibration constants such as the polarizer offset (P_o) and analyzer offset (A_o) values together with the attenuation constant (η) are obtained using the procedure

suggested by Aspnes[4], that is applicable to the present system with some minor adjustments to implement the correction terms given in Eqns. (14) and (15). A description of the calibration procedure with adjustments for the correction terms follows. The data measured at STO at several polarizer angles is used for the calculation of the spectra of correction terms vs wavelength at each polarizer angle according to Eqns. (14) and (15). For these calculations approximate values of P_o and A_o are input. With this correction term spectra, the experimental Fourier coefficients (either α_{sto} and β_{sto} or α_m and β_m) are converted into α and β using Eqns. (12) and (13). In addition to the well known residual calibration method, another calibration method using the phase information[8] is also performed in the present work and from here on is called an RAset method. It relies on the fact that the relative position of the analyzer starting angle to the polarizer zero point is fixed for a given hardware configuration of an RA type SE system. Also, the analyzer phase angle, $-(1/2)\tan(\beta_{sto}/\alpha_{sto})$, varies exactly the same amount as the change of the polarizer angle at STO. In another words, there is a linear relation with slope=1.0 and an one-to-one correspondence between the polarizer angle and the analyzer phase angle at STO. Since the slope(=1.0) and the y-intersection are independent of sample alignment, this line of $-(1/2)\tan(\beta_{sto}/\alpha_{sto})$ vs polarizer angle is adopted as a reference phase line for the RAset method of phase calibration. Once this reference line is available, the calibration constants are easily obtained since one more phase line is obtained as a part of the

residual calibration procedure. The intersection of that phase line with this reference phase line will yield the two calibration constants (P_o, A_o). The only requirement for the intersection between two phase lines to exist is that the phase line with a sample should not be parallel to the reference phase line, a condition which is always satisfied ($r_p \neq r_s$, with sample). This RAset method not only shares the same complimentary properties as the phase calibration when compared to the residual calibration but also has the additional benefit that it does not require extra measurements at around $P=P_o+90$ for each calibration. The only requirement is the STO measurement for the reference phase line. Once this reference phase line is obtained, it can be used with any phase line with a sample. Hence, while one does the residual calibration, this phase calibration method can be done simulataneously. Calibration constants are obtained both by the residual calibration and by the RAset phase calibration, and are plotted out versus wavelength. The programs regarding calibrations and the following analyses were done with FORTRAN77.

For the spectrum, the intensity variation vs the rotating analyzer is boxcar averaged over N_b mechnical turns of the rotating analyzer. This boxcar averaging is repeated N_f times and the Fourier coefficients are numerically filtered to remove erratic spikes and then averaged to yield (α_{2m}, β_{2m}) at each wavelength. With boxcar averaging and numerical filtering, it takes about an hour to get a spectrum with ~100 data points. Measurements and calibrations are mostly done at 70° incident angle (except STO) using a gold

film evaporated onto a glass slide or a bare c-Si wafer with native oxide. The experimentally obtained $(\alpha_{2m}, \beta_{2m})$ are converted into (α, β) and (Δ, ψ) using the calibration constants and the correction terms.

Correction Spectra

Spectra of the correction terms are calculated from the experimental spectra of α_{sto} and β_{sto} according to Eqns.(14) and (15). These correction terms will be zero for an ideal system, but a small deviation from zero is expected for a real system. The correction spectra are shown in Figures (2) and (3) for the present RA type SE system which display a wavelength dependence as well as a polarizer angle dependence. The spectra show two characteristic features. One is that the overall features of ξcos2F and ξsin2F remain the same, that is, the spectra remain parallel as the polarizer angle is varied. Also, the magnitude of the spectra is within a few percent. The rotation angle F is quite close to the polarizer angle P and ξ is small. $F=P+\delta P$ ($\delta P=0.05°$) and $\xi=0.0299$ are the best fit values to the correction specra. The finiteness of δP indicates that the possible rotation of the polarization axis inside the optical fiber is constant with respect to polarizer position. Also the rotation of the polarizaton axis is quite small (0.05°). The magnitude of ξ is about twice the residual at P_o. One realizes that the nonzero residual value originates from attenuation by the electronic circuit, and one of the attenuation effects on the Fourier coefficients (α and β) is the magnitude

change. This effect is corrected by multiplying the attenuation factor $(1/\eta)$ by the Fourier coefficients. The same effect of attenuation when viewed in light of the present correction terms are $(\xi\cos 2F)_\eta = (1-\eta)\cos 2P/(1-\eta/2)$ and $(\xi\sin 2F)_\eta = (1-\eta)\sin 2P/(1-\eta/2)$. Since the value of the attenuation factor η is 0.985 as measured by the residual calibration, $(\xi\cos 2F)_\eta \cong 0.0296\cos 2P$ and $(\xi\sin 2F)_\eta \cong 0.0296\sin 2P$, respectively, which agrees well with the previous result of $\xi = 0.0299$ and $F = P + 0.05°$. Hence it is verified that the correction to α and β according to the first feature observed in Figures (2) and (3), the parallel shift, is the same as that by the attenuation factor (η) correction in the residual calibration. The other characteristic feature observed in Figures (2) and (3) is the gradual change vs wavelength and a sharp dip (peak) centered around 640nm in the spectra of $\xi\cos 2F$ $(\xi\sin 2F)$. This feature is due to the grating (#1) inside the monochromator. When the second grating (#2) which has a different blaze wavelength and a different number of grooves/mm is used, a different feature is observed. This characteristic feature due to the grating (#1) is extracted by averaging the correction spectra $\xi\cos 2F$ and $\xi\sin 2F$ over all the polarizer angles, respectively. The averaging process will cancel out the correction components due to the first feature, since the measurements are done over one optical cycle of the analyzer angle in a uniform interval. The spectra of the correction terms characteristic of the second feature are presented in Figure (4).

Calibration constants

The spectra of P_o, the polarizer offset and A_o, the analyzer offset obtained with a Au film, are shown in Figures (5) and (6). It is interesting to compare the offset spectra by the two different calibration methods (residual calibration vs RAset phase calibration) and to see how these spectra change as the correction terms are applied. Using the residual calibration, the polarizer offset is almost constant with wavelength, and does not change significantly after correction. The correcton procedure reduces the scatter in the polarizer offset at longer wavelengths. However, P_o by the RAset phase calibration method gradually decreases as wavelength increases, and the maximum variation is as much as ~1.3°. This rather large variation of P_o almost disappears when the correction terms are introduced, and the P_o spectrum becomes nearly the same as that by residual calibration. On the other hand, A_o by either calibration method shows a strong wavelength dependence prior to correction. The maximum variation of A_o is as much as ~1.3. The sharp dip around 640nm is also clearly observed. After correction, A_o is rather flat and the dip at 640nm disappears, showing the improvements made by the correction terms. It should be mentioned that although the correction process removes most of spectral dependence of the calibration constants, there still remains some slight spectral dependence of A_o. This wavelength dependence of the offset constants are a direct consequence of several effects. Although the actual values of slope and y-

intersection of the best fit line to $(1/2)\tan(\beta/\alpha)$ vs polarizer angle shows negligible scattering from the ideal values, and the values of y-intersection show spectral behavior, this wavelength dependence of the y-intersection is the origin of the offset variation (P_o and A_o) vs wavelength. Since this wavelength dependence of the y-intersection is greatly reduced after the correction process, the same improvement in offset spectra is also observed. Post-correction spectra of P_o and A_o could be fit to straight lines. The best fit of P_o and A_o into straight lines gives $P_o = -0.237-0.00018\lambda$ (°, λ in nm), and $A_o = -52.57-0.00075\lambda$ (°, λ in nm), respectively.

The RA type SE with an optical fiber bundle detection system has many advantages. One major drawback is from an incomplete depolarization by the optical fiber, since the linear polarized light after reflections by the mirrors and the grating inside the monochromator, might alter the ellipsometric constants. The effect of this residual linear polarized light is measured. The correction is made via the introduction of the attenuation constant for the electronic circuit and the correction terms for the optical fiber bundle/grating. After the correction process, most of the spectral variation of the calibration constants are removed. A slight deviation from the ideal behavior, in the analyzer offset, Ao implies that further work is required to completely solve this problem.

Acknowledgement

The author (SYK) is on his leave from Ajou University, Suwon in Korea. He would like to acknowledge KOSEF and Ajou University for support of research through 1993. The research work was supported in part by the Office of Naval Research, ONR.

References

1. D.E. Aspnes, "New development in spectroellipsometry: the challenge of surfaces," Thin Solid Films, vol.233, 1-8 (1993).
2. E.A. Irene, "Application of spectroscopic ellipsometry to microelectronics," Thin Solid Films, vol.233, 96-111 (1993).
3. R.W. Collins, I. An, H.V. Nguyen and Y. Lu, "Real time spectroscopic ellipsometry for characterization of nucleation, growth, and optical functions of thin films," Thin Solid Films, vol.233, 244-252 (1993).
4. D.E. Aspnes, "Effect of component optical activity in data reduction and calibration of rotating-analyzer ellipsometers," J. Opt. Soc. Am., vol.64, 812-819 (1974).
5. D.E. Aspnes and A.A. Studna, "High precision scanning ellipsometers," Appl. Opt., vol.14, 220-228 (1975).
6. from the manual of SOPRA EG4G, 68 rue Pierre Joigneaux, F92270 Bois-Colombes, France.
7. from the manual of Rudolph S2000, 1 Rudolph Road, P.O. Box 1000, Flanders, NJ 07836, USA.

8. J.M.M. de Nijs, A.H.M. Holtslag, A. Hoeksta, and A. van Silfhout, "Calibration method for rotating-analyzer ellipsometers," J. Opt. Soc. Am. A, vol.5, 1466-1471 (1988).

Figure captions

Figure 1. A schematic diagram of rotating analyzer spectroscopic ellipsometer with a fiber optic detection system.

Figure 2. Spectra of the correction term ξcos2F at the polarizer angles of 90(✳), 75(■), 60(▲), 45(●), 30(▼), 15(◆), 0(+), -15(◇), -30(▽), -45(○), -60(△), and -75(□) degrees.

Figure 3. Spectra of the correction term ξsin2F at the polarizer angles of 90(✳), 75(■), 60(▲), 45(●), 30(▼), 15(◆), 0(+), -15(◇), -30(▽), -45(○), -60(△), and -75(□) degrees.

Figure 4. Spectra of the correction term ξcos2F and ξcos2F due to the grating #1.

Figure 5. Polarizer offset versus wavelength obtained with Au film, with (◆) and without (○:residual calibration, △:phase calibration) corrections.

Figure 6. Analyzer offset versus wavelength obtained with Au film, with (◆) and without (○:residual calibration, △:phase calibration) corrections.

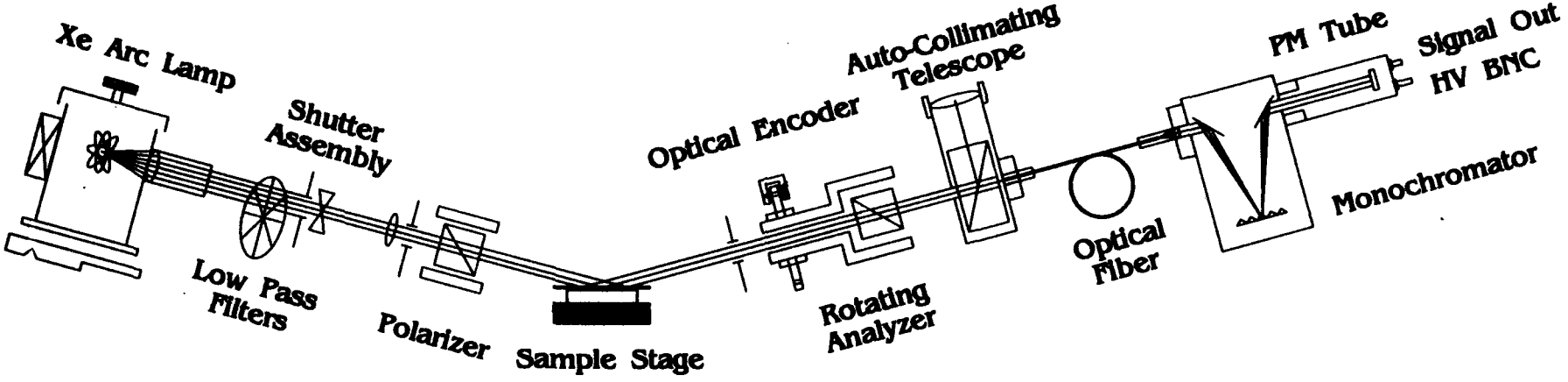

Figure 1. Schematic diagram of rotating analyzer spectroscopic ellipsometer with optical fiber detection system.

Fig.2 Spectra of the corrction term ξcos2F

SY Kim Applied Optics

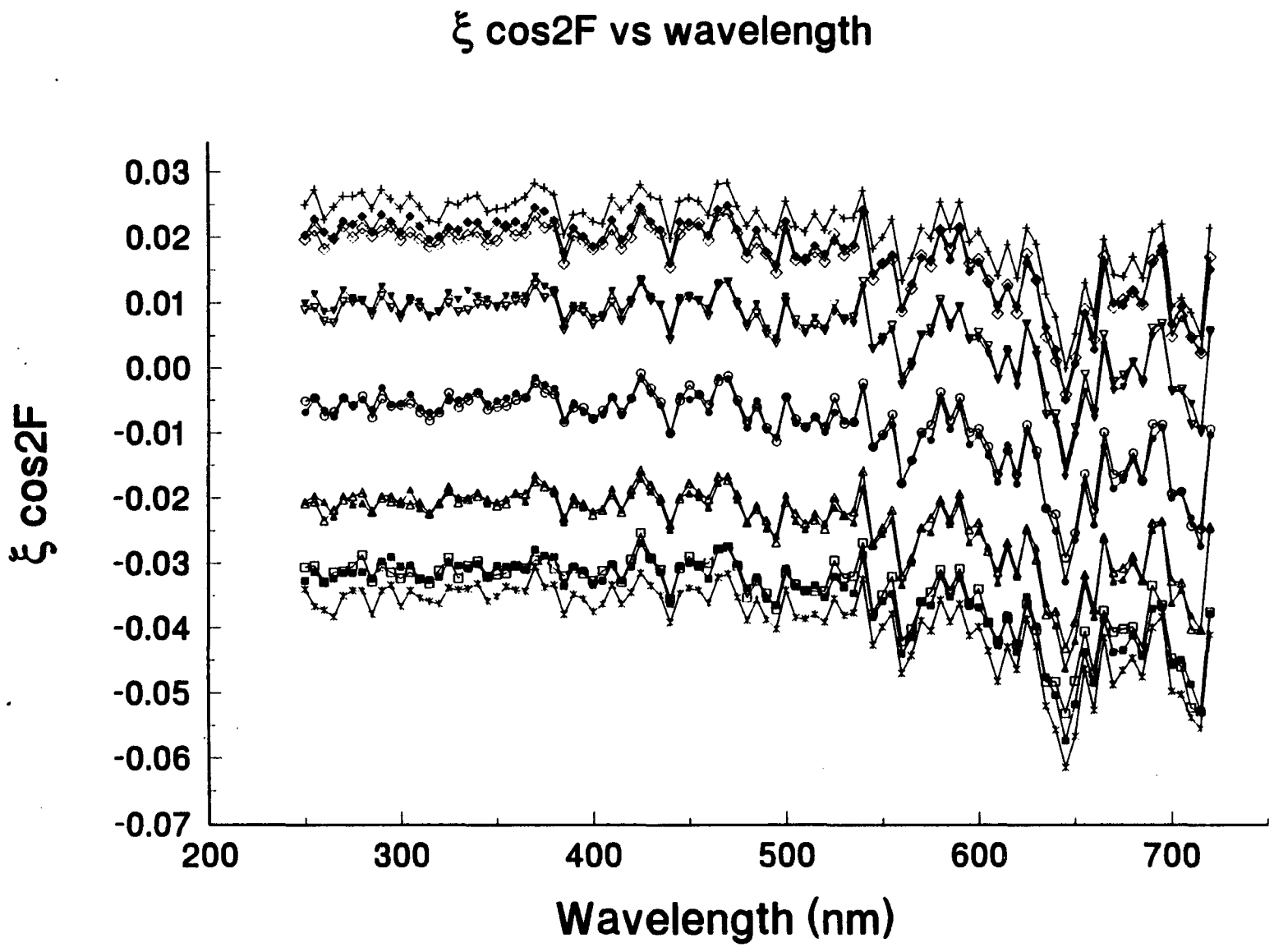

Fig.3 Spectra of the correction term ξsin2F

SY Kim Applied Optics

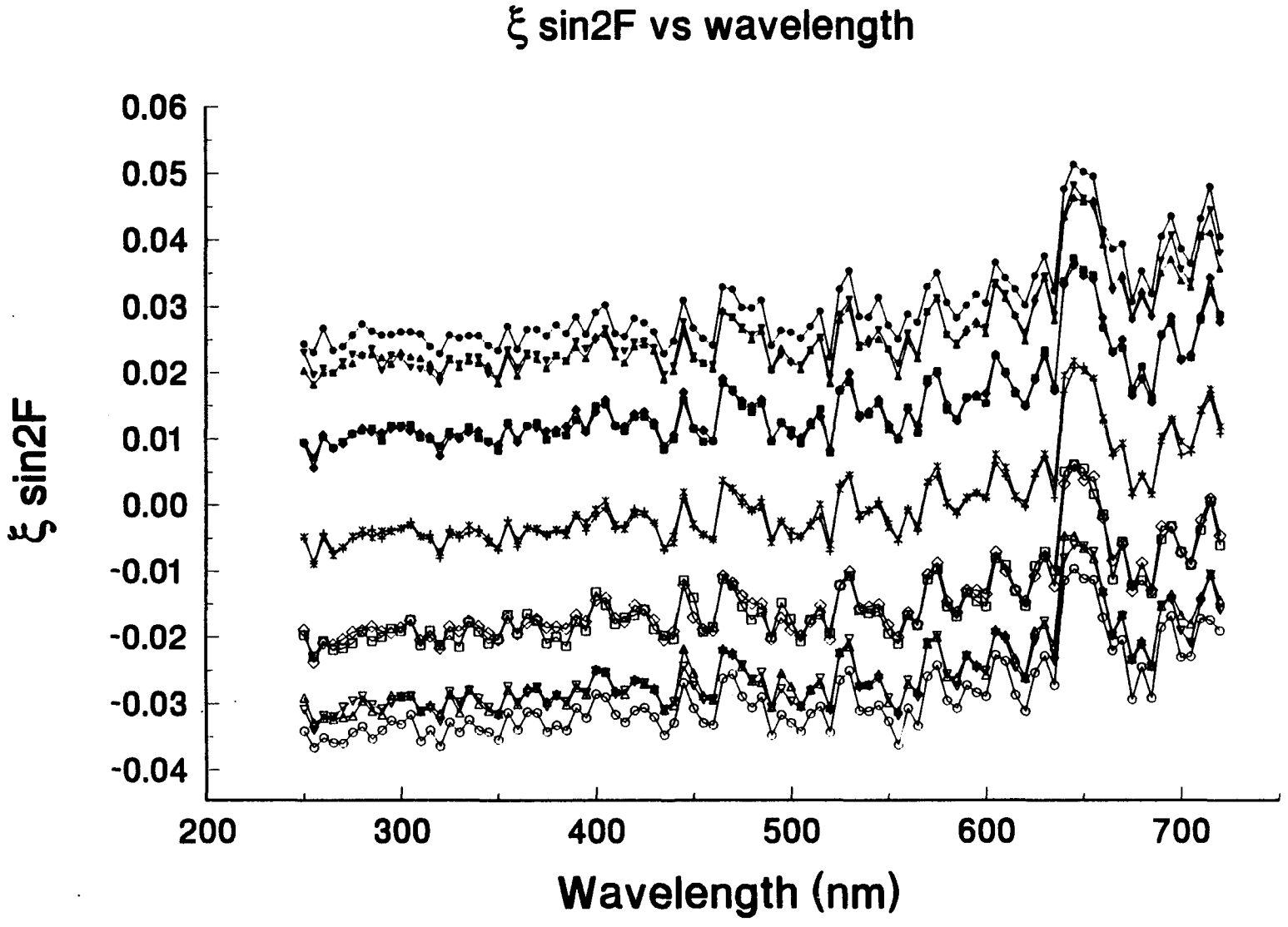

Fig.4 spectra of the correction terms

SY Kim Applied Optics

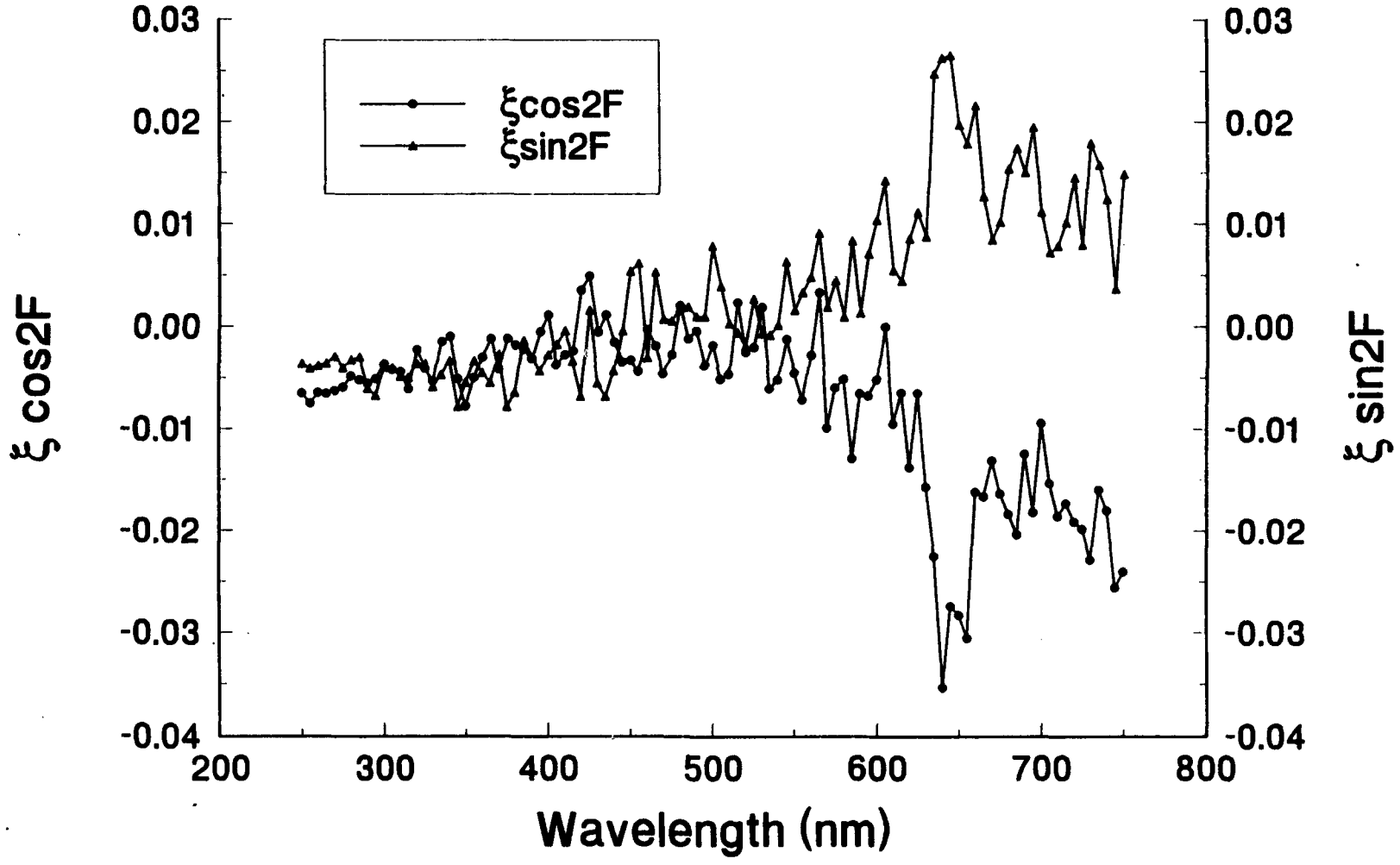

Figure 6 Analyzer offset vs wavelength

SY Kim, Applied Optics

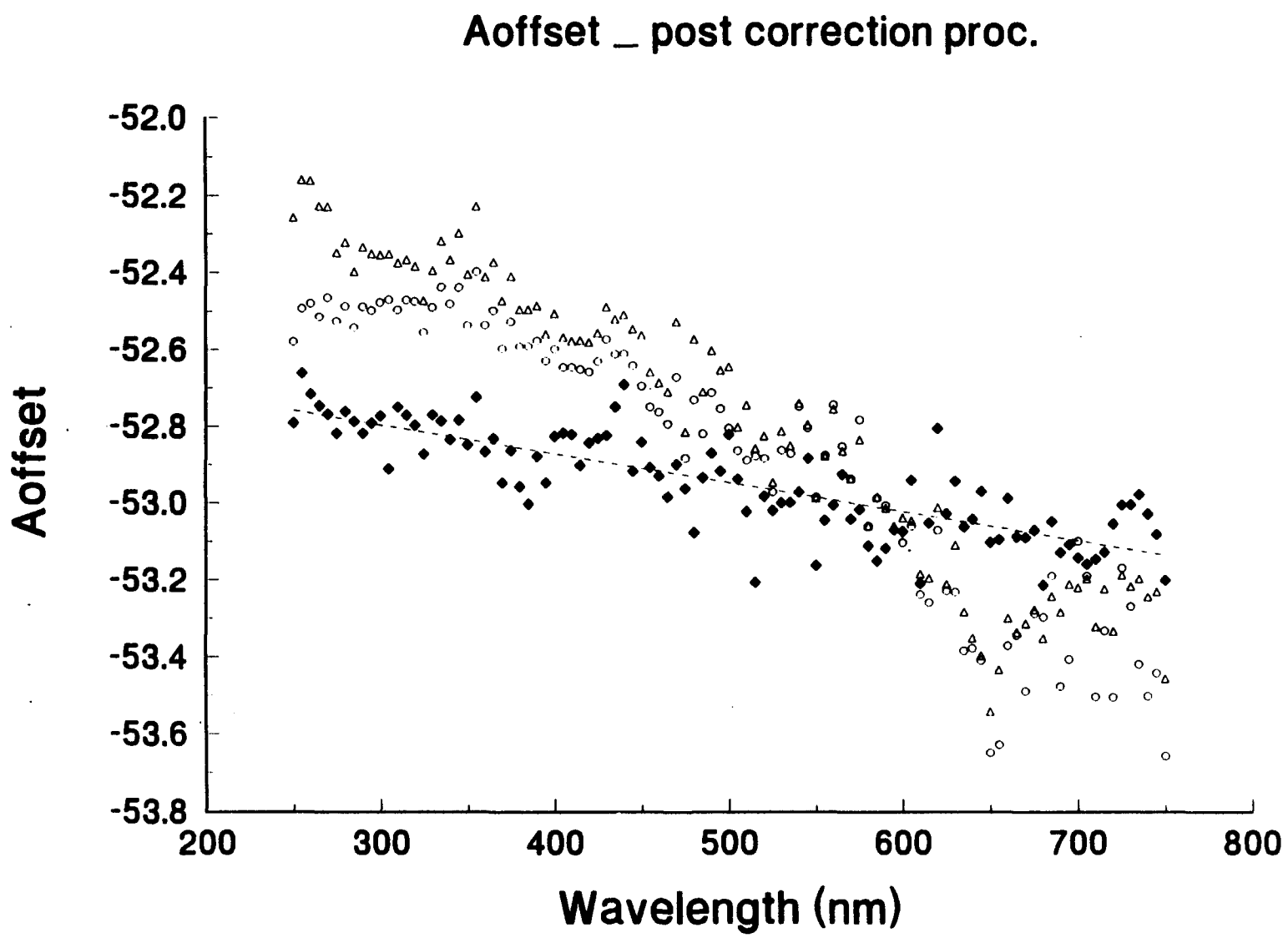

Figure 5 Polarizer offset vs wavelength

SY Kim Applied Optics